

Stereostructure Assignment of Medium-Sized Rings through an NMR–Computational Combined Approach. Application to the New Germacranes Ketopelenolides C and D

Ernesto Fattorusso,[†] Paolo Luciano,[†] Adriana Romano,[†] Orazio Tagliatela-Scafati,^{*,†} Giovanni Appendino,[‡] Marianna Borriello,[†] and Caterina Fattorusso[†]

Dipartimento di Chimica delle Sostanze Naturali, Università di Napoli “Federico II”, Via D. Montesano 49, 80131, Naples, Italy, and Dipartimento di Scienze Chimiche, Alimentari, Farmaceutiche e Farmacologiche, Università del Piemonte Orientale, Via Bovio 6, 28100 Novara, Italy

Received June 16, 2008

The new germacranes ketopelenolides C (**2**) and D (**3**) have been isolated from great mugwort (*Artemisia arborescens*). Their stereostructure elucidation exemplifies some of the most common pitfalls facing the configurational assignment of medium-sized polyfunctionalized compounds. It was established through a combined strategy including chemical derivatization, NMR data analysis, molecular modeling, and quantum-mechanical calculations including a comparison between experimental ¹³C NMR data and a Boltzmann-weighted average of DFT-calculated ¹³C NMR chemical shifts.

The configurational assignment of natural products containing flexible medium-sized rings presents unique challenges compared to acyclic and other cyclic compounds. Indeed, similarly to acyclic compounds, the flexibility of many medium-range rings makes the interpretation of scalar couplings difficult to translate in conformational terms, while, compared to other cyclic systems, where one or only a very limited number of conformations exist, several families of conformations are reasonably populated in medium-sized compounds and should all be taken into account to translate dipolar couplings into configurational relationships. Consequently, in these cases, a detailed analysis of the conformational behavior should be considered mandatory to minimize the risks of stereostructural misassignments. The advanced computational techniques now available have made it possible also to complement the NMR analysis with quantum-mechanical prediction of ¹³C NMR chemical shifts,¹ through *ab initio* calculations of electronic distribution. The consistency of results obtained from investigation of NOE contacts, molecular mechanics, and quantum-mechanical calculation of ¹³C NMR data strongly supports the assignment of the relative configuration.

We have recently applied these concepts to the configurational analysis of the *nor*-caryophyllane artarborol (**1**)² (Chart 1) and have now used the more densely functionalized ketopelenolides C (**2**) and D (**3**) (Chart 1) as probes to assess the applicability of this strategy also to germacranolide derivatives.^{3,4}

Ketopelenolides C (**2**) and D (**3**) were obtained from the great mugwort (*Artemisia arborescens* L., Asteraceae, tribe Anthemidae), an evergreen shrub endemic to the Mediterranean area that presents several features to justify a systematic study of its secondary metabolites. Indeed, the essential oil of *A. arborescens* has the highest amount of chamazulene of any essential oil known (up to 40%), and the plant is a prolific producer of bitter sesquiterpene lactones, two of which, the guaianolides arborescin (**4**)⁵ and matricin (**5**)⁶ (Chart 2), are currently used as starting material for our ongoing studies on the mechanism of bitter taste.⁷

Results and Discussion

Ketopelenolides C (**2**) and D (**3**) were obtained from side-cuts of the large-scale chromatographic purification of **4** and **5**. Thus, the aerial parts of *A. arborescens* were extracted with acetone at rt to give a black gum, which was next partitioned between H₂O and

Chart 1

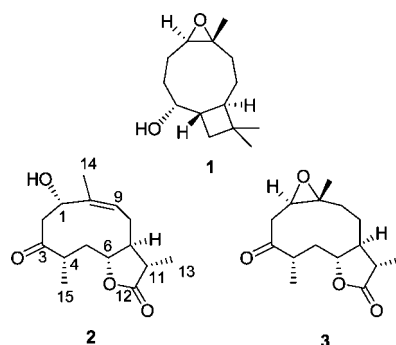
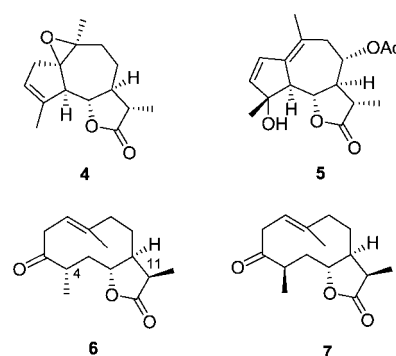


Chart 2



EtOAc. The organic phase was chromatographed over a silica column using a gradient solvent of increasing polarity. Two abundant and pure fractions were identified as arborescin (**4**) and matricin (**5**), respectively. Arborescin (**4**) has been widely investigated due to its key role in the generation of azulenoid compounds during steam distillation of plant biomasses,⁸ however, its reported NMR data are largely incomplete;⁹ a detailed assignment of NMR data is provided in the Experimental Section. A fraction eluted with EtOAc/*n*-hexane (6:4) was further purified by normal-phase HPLC (eluent: *n*-hexane/EtOAc, 55:45) to give ketopelenolides C (**2**, 0.02%) and D (**3**, 0.03%) as colorless, amorphous solids.

Ketopelenolide C (**2**) gave a molecular ion peak at *m/z* 266.1523 in the HREIMS, corresponding to the molecular formula C₁₅H₂₂O₄, which implies five unsaturation degrees. These mass data and, above all, 1D (¹H and ¹³C) NMR spectra of **2** (CDCl₃, Table 1) suggested that this compound was a sesquiterpene lactone. In particular, one methyl singlet (δ_{H} 1.86) and two methyl doublets (δ_{H} 1.19 and

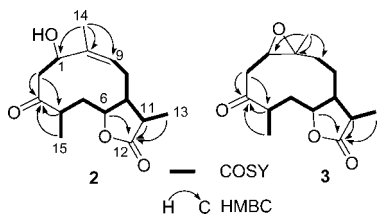
* To whom correspondence should be addressed. Phone: +39 081 678509. Fax: +39 081 678 552. E-mail: scatagli@unina.it.

[†] Università di Napoli “Federico II”.

[‡] Università del Piemonte Orientale.

Table 1. ^{13}C (125 MHz) and ^1H (500 MHz) NMR Data of Ketopelenolides C (**2**) and D (**3**) (in CDCl_3)

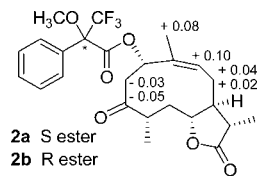
pos.	ketopelenolide C (2)		ketopelenolide D (3)	
	δ_{C} , mult.	δ_{H} (mult., J in Hz)	δ_{C} , mult.	δ_{H} (mult., J in Hz)
1	68.0, CH	4.97 (ddd, 10.7, 3.2, 1.5)	58.8, CH	3.27 ^a
OH-1		1.68 (d, 1.5)		
2a	43.2, CH ₂	2.96 (t, 10.7)	42.8, CH ₂	3.30 ^a
2b		2.60 ^a		2.35 ^a
3	211.5, qC		208.7, qC	
4	46.8, CH	2.62 ^a	45.3, CH	2.82 (h, 6.8)
5a	37.0, CH ₂	2.22 (m)	39.6, CH ₂	2.22 ^a
5b		1.83 ^a		1.85 (dt, 13.0, 6.5)
6	81.8, CH	4.02 (ddd, 10.0, 10.0, 2.2)	82.6, CH	4.03 (m)
7	49.3, CH	1.88 (ddd, 10.0, 9.5, 8.5)	51.9, CH	1.70 ^a
8a	30.2, CH ₂	2.37 ^a	29.5, CH ₂	2.33 ^a
8b		2.01 (dd, 13.8, 2.6)		1.98 (m)
9a	121.2, CH	5.34 (dd, 12.0, 2.6)	38.3, CH ₂	1.68 ^a
9b				1.22 ^a
10	138.2, qC		60.3, qC	
11	41.9, CH	2.39 ^a	43.5, CH	2.27 ^a
12	177.3, qC		177.5, qC	
13	13.7, CH ₃	1.19 (d, 7.5)	14.9, CH ₃	1.28 (d, 7.0)
14	18.2, CH ₃	1.86 (bs)	16.9, CH ₃	1.40 (s)
15	18.8, CH ₃	1.12 (d, 7.5)	17.0, CH ₃	1.24 (d, 6.5)

^a Overlapped with other signals.**Figure 1.** COSY and key HMBC correlations for ketopelenolides C (**2**) and D (**3**).

1.12) were evident in the ^1H NMR spectrum, while the presence of one ketone carbonyl (δ_{C} 211.5) and one ester carbonyl (δ_{C} 177.3) was disclosed by inspection of the ^{13}C NMR spectrum. The 2D HSQC spectrum was then used to associate all the proton signals to the corresponding carbon signals and evidenced the presence of two oxygenated methines (δ_{C} 81.8, δ_{H} 4.02; δ_{C} 68.0, δ_{H} 4.97) and one trisubstituted double bond (δ_{C} 121.2, δ_{H} 5.34; δ_{C} 138.2). The three multiple bonds resulting from the above analysis left unassigned two of the unsaturation degrees, indicating, consequently, that compound **2** is bicyclic.

Analysis of the COSY spectrum of **2** made it possible to sort all the proton multiplets into two spin systems (shown in bold in Figure 1), while inspection of the $^{2,3}J_{\text{C-H}}$ correlation peaks evidenced through the 2D HMBC spectrum (most important correlations are depicted in Figure 1) joined the above deduced moieties, defining the atom connectivity of ketopelenolide C (**2**). In particular, the correlations of both H-6 and H-11 (δ_{H} 2.39) with the ester carbonyl were indicative of the presence of a γ -lactone moiety. Correlation peaks of the methyl singlet at δ_{H} 1.86 (C-14) with C-1, C-9, and C-10 established the first connection point among the two spin systems, while the correlations of H₂-2 (δ_{H} 2.60 and 2.96), H-4, and H₃-15 with the signals at δ_{C} 211.5 identified the ketone carbonyl as the second connection point. Thus, the 10-membered macrocyclic ring of the germacranes derivative ketopelenolide C (**2**) was completely defined. The spatial proximity of H-9 with H₃-14, evidenced through the ROESY spectrum of **2**, indicated the Z configuration of the endocyclic double bond.

Ketopelenolide D (**3**), $\text{C}_{15}\text{H}_{22}\text{O}_4$ by HREIMS, has the same molecular formula as ketopelenolide C (**2**). Comparison of 1D NMR spectra (^1H and ^{13}C) of **3** with parallel spectra of **2** suggested a close similarity between these two compounds. Indeed, the only significant differences were the lack of ^1H and ^{13}C NMR signals of the $\Delta^{9,10}$ double bond in **3**, which, in turn, exhibited the signal

**Figure 2.** Applications of the modified Mosher's method for ketopelenolide C. $\Delta\delta(S - R)$ are given in ppm.

of an additional oxygenated and unprotonated carbon atom (δ_{C} 60.3, C-10). Furthermore, the singlet of the methyl group presumably linked to this carbon appeared high-field shifted in the ^1H NMR spectrum of **3** (δ_{H} 1.40 instead of 1.86). The combined inspection of 2D NMR spectra (COSY, HSQC, and HMBC) led to the unambiguous assignment of all the ^1H and ^{13}C NMR resonances and the definition of the ketopelenolide D (**3**) backbone. Figure 1 shows that the two spin systems evidenced from the COSY spectrum of **3** are closely related to those previously evidenced for compound **2**. Likewise, the presence of the γ -lactone moiety and the attachment of the two spin systems to the ketone carbonyl was deduced by similar $^{2,3}J_{\text{C-H}}$ HMBC correlation peaks. On the other hand, the methyl at δ_{H} 1.40 showed HMBC correlation peaks with the methylene carbon C-9 (δ_{C} 38.3; δ_{H} 1.68 and 1.22) and with two oxygenated carbons, C-1 (δ_{C} 58.8, δ_{H} 3.27) and C-10 (δ_{C} 60.3). These correlations are strongly indicative of the presence of an epoxide ring, further supported by the characteristic relatively high-field resonances of these carbons. The presence of this additional oxygen-containing ring also accounts for the remaining unsaturation degree. The atom connectivity of the epoxide-containing germacranes lactone ketopelenolide D (**3**) was therefore completely defined.

Assignment of the correct configuration at the five stereogenic carbon atoms of ketopelenolide C (**2**) and at the six stereogenic carbon atoms of ketopelenolide D (**3**) was next attempted. An analysis of literature data in search of configurational similarities was of little avail. Indeed, ketopelenolides A (**6**)¹⁰ and B (**7**)¹¹ (Chart 2), two compounds related to **2** and **3**, are diastereomeric at C-4; in addition, a number of different configurational arrangements at the three stereogenic centers of the lactone ring (C-6, C-7, and C-11) have been reported for germacranes and related sesquiterpene lactones, as exemplified also by compounds **4** and **5** (see differences of configuration at C-11 with **6** and **7**). Therefore, ketopelenolides C (**2**) and D (**3**) qualified as ideal targets to exploit our strategy for the assignment of relative configuration to medium-range macrocycles, based on the combined application of NMR, molecular modeling, and quantum-mechanical calculations, that we had successfully developed for the nine-membered ring of artarborol (**1**).²

Starting with the relatively more simple case of ketopelenolide C (**2**), since this compound is a secondary alcohol, application of the modified Mosher's method¹² could establish the absolute configuration at the hydroxymethine carbon. To this aim, two aliquots of ketopelenolide C (**2**) were dissolved in dry pyridine and allowed to react overnight with (*R*)- and (*S*)-MTPA chloride, affording the (*S*)- and (*R*)-MTPA esters **2a** and **2b**, respectively (Figure 2). Analysis of the $\Delta\delta(S - R)$ values according to the Mosher's model (Figure 2) pointed to the *S* configuration at C-1 of **2**.

A further reduction of the number of possible stereoisomers of **2** was obtained by analysis of NOE contacts (evidenced by cross-peaks of the 2D NMR ROESY spectrum) around the γ -lactone ring. Thus, the cross-peak H-6/H-11 pointed to a *cis* orientation of these protons, while both cross-peaks H-7/H₃-13 and H-6/H-8a indicated the relative orientation at C-7.

Consequently, only the four stereoisomers **C1**–**C4**, shown in Figure 3, remained as possible candidates for the final structure. As discussed above, only a detailed knowledge of the conformational behavior of these stereoisomers could allow an unambiguous

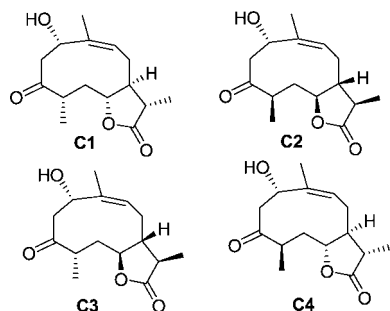


Figure 3. The four possible stereoisomeric candidates for the structure of ketopelenolide C.

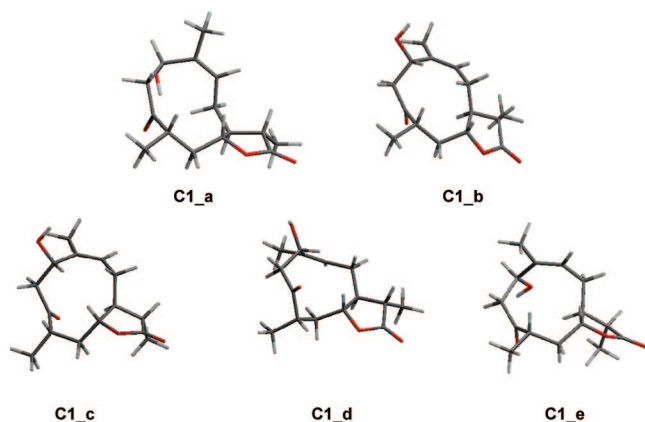


Figure 4. The major conformational families for stereoisomer C1. Conformational families for stereoisomers C2, C3, and C4 are provided as Supporting Information.

analysis of additional NOE couplings of the entire molecule and their translation in terms of configuration.

To this aim, the four possible stereoisomers were subjected to conformational search using the Simulated Annealing procedure, with atomic potentials and charges assigned by the *cff91* force field. The conformational space of the compounds was sampled through 200 cycles of Simulated Annealing: an initial temperature of 1000 K was applied to the system and then linearly reduced to 300 K. The resulting structures were subjected to energy minimization until the maximum root-mean-square (rms) derivative was less than 0.001 kcal/Å. To simulate the solvent chosen for NMR analysis, a distance-dependent dielectric constant set to the value of CHCl₃ (ϵ 4.8) was used during the calculations. Resulting conformers were ranked on the basis of their conformational energy values and grouped into families according to their 10-membered-ring dihedral angles values. This analysis confirmed the flexibility of the 10-membered ring of germacrane derivatives, as indicated by the number of major conformational families obtained for the four different stereoisomers: C1 (5 families), C2 (7 families), C3 (5 families), C4 (7 families) (Figure 4 and Supporting Information).

In order to investigate the electronic distribution of the obtained conformers and the geometry more consistent with it, the lowest energy conformation of each family was subjected to a full geometry optimization by semiempirical calculations, using the AM1 method (Mopac 6.0 package in Ampac/Mopac module of Insight 2000.1). The obtained geometries were further optimized at the density functional theory (DFT) level (see below). This complex set of conformations was subsequently analyzed in light of two intense ROESY cross-peaks between H-1 and H-4 and between H-4 and H-6, resulting from the transannular proximity of these two protons. Since only C1 exhibited at least one reasonably populated family of conformations showing the required distance (about 2.5 Å) and accessibility for both H-1/H-4 and H-4/H-6 (a comprehensive table

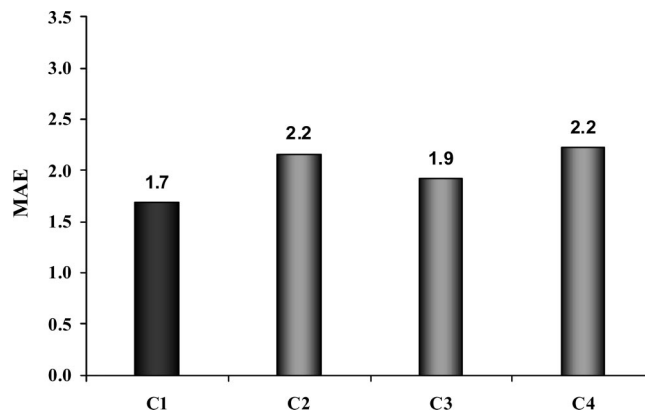


Figure 5. Mean absolute error ($\sum[|\delta_{\text{exp}} - \delta_{\text{calcd}}|]/n$) relative to stereoisomers C1–C4, in $\Delta\delta$ (ppm) units.

with interproton distances is reported as Supporting Information), we confidently assigned structure C1 to ketopelenolide C.

This stereochemical assignment was supported by employment of the recent methodology based on the quantum-mechanical prediction of ¹³C NMR chemical shifts.¹ ¹³C NMR chemical shifts are preferred to ¹H NMR resonances, whose prediction is also feasible, in light of their larger spectral window. Among the different computational possibilities, the gauge including atomic orbitals (GIAO) calculation of ¹³C NMR chemical shifts through the *ab initio* DFT method using the 6-31G(d,p) basis set¹³ proved to give very good results with artarborol (1);² and therefore, we applied it also to predict ¹³C NMR resonances of ketopelenolide C (2). Given the flexibility of the macrocyclic ring system of ketopelenolide C, the *ab initio* calculations were applied to each of the previously determined minimum energy families of conformers for each of the four possible stereoisomers C1–C4 (see above). Thus, in the case of 2, 24 different conformations were analyzed separately, their geometries were fully optimized, and the ¹³C NMR chemical shifts were calculated at the same level with the GIAO option using the MPW1PW91/6-31G(d,p) DFT method.¹⁴ Obtained results are collected in the Supporting Information. Inspection of these data, in comparison with experimental values of ¹³C NMR resonances, evidenced a systematic error for the carbonyl carbon C-12, whose ¹³C NMR resonance was severely underestimated for all four stereoisomers. Given the reported lack of efficiency of the above methodology to calculate ¹³C NMR resonances of sp² carbons,¹⁵ especially those resonating in the range 140–220 ppm, this kind of error was quite expected.

Thermochemical calculations at the same *ab initio* level in the harmonic approximation of the vibrational modes allowed the evaluation of the standard Gibbs free energy for all 24 conformers, at the NMR recording temperature of 298 K. Then, a Boltzmann-weighted average of ¹³C NMR chemical shifts for any given carbon atom of low-energy conformers was calculated separately for each of the four stereoisomers C1 to C4, using the *ab initio* standard free energies as weighting factors.¹⁶

All these calculations were carried out using the Gaussian03 program (see Supporting Information for details) and took approximately 24 h for each conformer, using a standard computer with a Pentium 4 processor.

In order to evaluate which of the four stereoisomers C1–C4 best fits with the experimental data, the experimental shifts were plotted against the calculated shifts and the least-squares fit values of slope, intercept, and correlation factor (r^2) were determined. Difference plots were determined by subtracting the so corrected chemical shifts from the experimental chemical shifts. In Figure 5 we report the mean absolute error (MAE = $\sum[|\delta_{\text{exp}} - \delta_{\text{calcd}}|]/n$) for each stereoisomer, expressed in $\Delta\delta$ units (during the MAE calculation carbon C-12 values were excluded). The lowest value

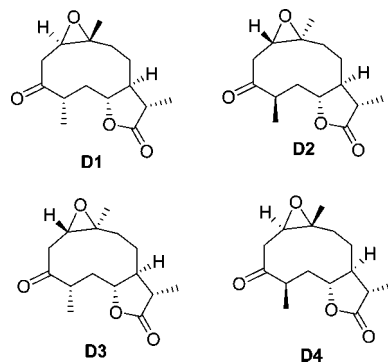


Figure 6. The four possible stereoisomeric candidates for the structure of ketopelenolide D.

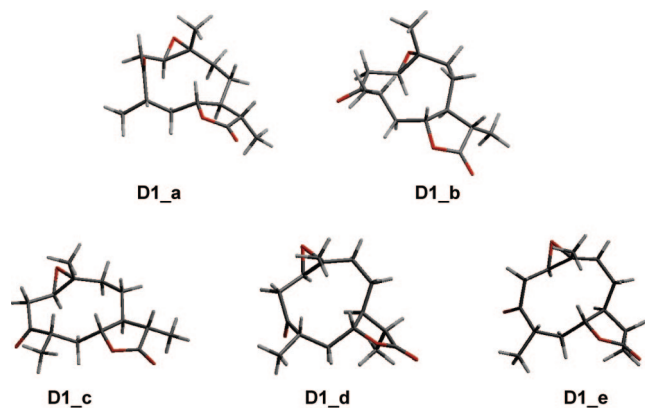


Figure 7. The major conformational families for stereoisomer **D1**. Conformational families for stereoisomers **D2**, **D3**, and **D4** are provided as Supporting Information.

of 1.69 ppm for **C1** clearly puts in evidence the better agreement between the chemical shifts calculated for the stereoisomer **C1** and the experimental values, compared to all the other stereoisomers. Therefore, the results of *ab initio* calculations are in full agreement and give support to the previous assignment of structure **C1** to ketopelenolide **C** (2).

The same NMR-computational approach detailed for ketopelenolide **C** (2) was used to assign the relative configuration to the epoxide-containing ketopelenolide **D** (3). Also in this case, some unambiguous NOE contacts around the three- and the five-membered rings (evidenced through the 2D ROESY experiment) were instrumental to reduce the number of possible stereoisomers. In particular, correlations H-6/H-11, H-7/H₃-13, and H-6/H-8a indicated the relative orientation of the five-membered ring, while the correlation H₃-14/H-2a was indicative of the *trans* geometry of the epoxide ring. Thus, the four relative orientations **D1–D4**, shown in Figure 6, could be possible for the structure of ketopelenolide **D**. As described above for ketopelenolide **C**, these four stereoisomeric molecules were subjected to conformational search, and then the resulting conformers were pooled into families (according to the 10-membered-ring conformation), ranked on the basis of their conformational energy values, and geometries were optimized at the DFT level. The following number of major families was obtained for the four different stereoisomers: **D1** (5 families), **D2** (7 families), **D3** (4 families), **D4** (5 families) (Figure 7 and Supporting Information).

The four intense ROESY cross-peaks H-1/H-7, H₃-14/H-6, H₃-14/H-4, and H-4/H-6 were used to analyze, in terms of distance and accessibility, this set of conformations. As a result, the structure **D1** was assigned to ketopelenolide **D**.

This assignment was fully supported by GIAO quantum-mechanical calculation of ¹³C NMR chemical shifts performed by

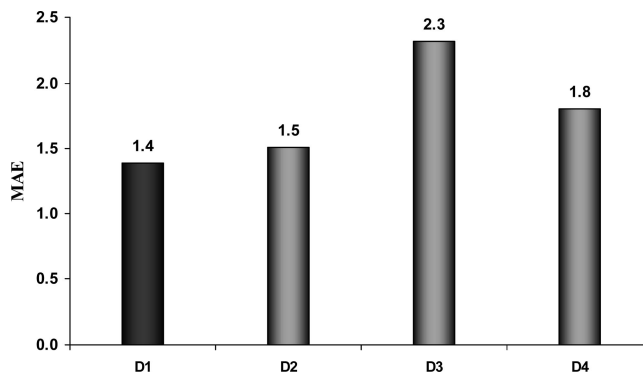


Figure 8. Mean absolute error ($\sum[|\delta_{\text{exp}} - \delta_{\text{calcd}}|]/n$) relative to stereoisomers **D1–D4**, in $\Delta\delta$ (ppm) units.

following the procedure described for ketopelenolide **C**. Briefly, the 21 different conformations were analyzed separately, their geometries were fully optimized, and the NMR chemical shifts were calculated (see Supporting Information). A Boltzmann-weighted average of ¹³C NMR chemical shifts for any remaining carbon atom of low-energy conformers, using the *ab initio* standard free energies as weighting factors, was calculated separately for each of the four stereoisomers **D1–D4** (see Supporting Information). The mean absolute error relative to each stereoisomer, calculated by subtracting corrected calculated chemical shifts from the experimental ones and expressed in $\Delta\delta$ units, is reported in Figure 8. In this case, the values of both the carbonyl carbons C-3 and C-12 were excluded due to the systematic error evidenced for their calculation. The better agreement with experimental data was obtained for stereoisomer **D1** (MAE = 1.39), although in this case another structure, namely, **D2**, also exhibited a good agreement (MAE = 1.50). Therefore, *ab initio* calculations and NMR analysis concur to assign structure **D1** to the natural sesquiterpene lactone ketopelenolide **D** (3). It should be noted that, in the case of ketopelenolide **D**, structure **D1** represents only the relative configuration of the compound, since its absolute configuration has not been determined.

A growing body of evidence suggests that the *ab initio* prediction of ¹³C NMR chemical shifts is destined to become a critical strategy to support the stereostructural assignment of natural products. The full consistency between the spectroscopic analysis and the quantum-mechanical prediction of ¹³C NMR chemical shifts we obtained during our recent investigation on the *nor*-caryophyllane derivative artarborol (1),² as well as throughout the present work on the even more flexible germacranes ketopelenolides **C** (2) and **D** (3), provides the first evidence about the applicability of this computational technique for compounds having nonrigid medium-sized rings. Although it needs to be further validated with larger sets of molecules, this technique has significant potential, on account of the large number of naturally occurring compounds characterized by medium-sized rings, such as humulane, cembrane, jathrophane, briarane terpenoids, and many others.

Experimental Section

General Experimental Procedures. Optical rotations (CHCl₃) were measured at 589 nm on a Perkin-Elmer 192 polarimeter equipped with a sodium lamp ($\lambda = 589$ nm) and a 10 cm microcell. ¹H (500 MHz) and ¹³C (125 MHz) NMR spectra were measured on a Varian INOVA spectrometer. Chemical shifts were referenced to the residual solvent signal (CDCl₃: δ_{H} 7.26, δ_{C} 77.0). Homonuclear ¹H connectivities were determined by the COSY experiment. One-bond heteronuclear ¹H–¹³C connectivities were determined with the HSQC experiment. Two- and three-bond ¹H–¹³C connectivities were determined by HMBC experiments optimized for a ^{2,3}J of 9 Hz. Through-space ¹H connectivities were evidenced using a ROESY experiment with a mixing time of 500 ms. Low- and high-resolution EIMS spectra (70 eV) were performed on a VG Prospec (Fisons) mass spectrometer. ESIMS spectra were performed on LCQ Finnigan MAT mass spectrometer. Medium-pressure

liquid chromatography was performed on a Büchi apparatus using a silica gel (230–400 mesh) column. HPLC were achieved on a Knauer apparatus equipped with a refractive index detector and LUNA (Phenomenex) SI60 (250 × 4 mm) columns.

Plant Material, Extraction, and Isolation. Powdered, nonwoody, dried plant material (500 g) collected at Cala Mosca, Cagliari (Italy), was extracted with acetone at rt (2 × 3 L). After removal of the solvent, 26 g of a black gum was obtained. This was dissolved in MeOH and vacuum-filtered through a bed of RP 18 silica gel (80 g) to afford 19 g of a dark orange paste, which was defatted by dissolving in MeOH (400 mL) and cooling. After removal of the abundant waxy precipitate, the filtrate was evaporated to afford 12.2 g of a gummy residue, which was fractionated by gravity column chromatography on silica gel (60 g) using a *n*-hexane/EtOAc gradient. The fractions eluting before arborescin (**4**, 2.9 g) were further purified by normal-phase HPLC (eluent: *n*-hexane/EtOAc, 55:45) to give ketopelenolide C (**2**, 0.1%) and ketopelenolide D (**3**, 0.1%) as colorless, amorphous solids.

Arborescin (4): colorless, amorphous solid; $[\alpha]_D^{25} +55$ (*c* 0.01, MeOH); $^1\text{H NMR}$ (500 MHz, CDCl_3) δ 5.57 (1H, H-3, bs); 4.02 (1H, H-6, t, *J* = 10.0 Hz); 2.83 (1H, H-5, bd, *J* = 10.0 Hz); 2.77 (1H, H-2a, bd, *J* = 16.1 Hz); 2.21 (1H, H-11, q, *J* = 7.0 Hz); 2.15 (1H, H-2b, bd, *J* = 16.1 Hz); 2.14 (1H, H-9a, overlapped); 1.95 (3H, H₃-15, s); 1.94 (1H, H-9b, overlapped); 1.64 (1H, H-8a, m); 1.47 (1H, H-8b, m); 1.35 (1H, H-7, overlapped); 1.35 (3H, H₃-14, s); 1.21 (3H, H₃-13, q, *J* = 7.0 Hz); $^{13}\text{C NMR}$ (125 MHz, CDCl_3) δ 178.8 (C-12, s); 140.6 (C-4, s); 124.6 (C-3, d); 82.6 (C-6, d); 72.4 (C-1, s); 62.5 (C-10, s); 54.5 (C-11, d); 52.3 (C-5, d); 40.9 (C-7, d); 39.5 (C-2, t); 33.5 (C-9, t); 22.7 (C-14, q); 22.6 (C-8, t); 18.1 (C-15, q); 12.4 (C-13, q); ESIMS (positive-ion) *m/z* 271 [M + Na]⁺, 521 [2M + Na]⁺; HREIMS *m/z* 248.1420 (calcd for C₁₅H₂₀O₃, *m/z* 248.1412).

Ketopelenolide C (2): colorless, amorphous solid; $[\alpha]_D^{25} -12$ (*c* 0.1, CHCl_3); $^1\text{H NMR}$ (500 MHz, CDCl_3) and $^{13}\text{C NMR}$ (125 MHz, CDCl_3) see Table 1; ESIMS (positive-ion) *m/z* 289 [M + Na]⁺; HREIMS *m/z* 266.1523 (calcd for C₁₅H₂₂O₄, *m/z* 266.1518).

Ketopelenolide D (3): colorless, amorphous solid; $[\alpha]_D^{25} -29$ (*c* 0.1, CHCl_3); $^1\text{H NMR}$ (500 MHz, CDCl_3) and $^{13}\text{C NMR}$ (125 MHz, CDCl_3) see Table 1; ESIMS (positive-ion) *m/z* 289 [M + Na]⁺; HREIMS: *m/z* 266.1511 (calcd for C₁₅H₂₂O₄, *m/z* 266.1518).

Preparation of MTPA Esters of Ketopelenolide C. Compound **2** (1 mg) was dissolved in 0.5 mL of dry pyridine, treated with (–)-*R*-MTPA chloride (15 μL) and 4-DMAP (a spatula tip), and maintained at rt under stirring overnight. After removal of the solvent, the reaction mixture was purified by HPLC on a SI60 column (*n*-hexane/EtOAc, 9:1), affording pure (*S*)-MTPA ester **2a** (1.1 mg). Using (+)-*S*-MTPA chloride, the same procedure afforded (*R*)-MTPA ester **2b** in the same yield.

Ketopelenolide C-1-O-(S)-MTPA ester (2a): amorphous solid; $^1\text{H NMR}$ (500 MHz, CDCl_3) δ 7.35 and 7.45 (MTPA phenyl protons); 5.38 (H-9, overlapped); 5.36 (H-1, overlapped); 4.04 (H-6, ddd, *J* = 10.0, 10.0, 2.2 Hz); 3.55 (MTPA OCH₃, s); 3.05 (H-2a, t, *J* = 10.5 Hz); 2.72 (H-2b, dd, *J* = 10.7, 3.2 Hz); 2.65 (H-4, m); 2.39 (H-11, overlapped); 2.37 (H-8a, overlapped); 2.25 (H-5a, m); 2.01 (H-8b, dd, *J* = 13.8, 2.6 Hz); 1.91 (H₃-14, bs); 1.88 (H-5b, overlapped); 1.88 (H-7, overlapped); 1.19 (H₃-13, d, *J* = 7.5 Hz); 1.14 (H₃-15, d, *J* = 7.5 Hz); FABMS (glycerol matrix, positive ions) *m/z* 483 [M + H]⁺.

Ketopelenolide C-1-O-(R)-MTPA ester (2b): amorphous solid; $^1\text{H NMR}$ (500 MHz, CDCl_3) δ 7.55 and 7.33 (MTPA phenyl protons); 5.35 (H-1, dd, *J* = 10.7, 3.2 Hz); 5.28 (H-9, dd, *J* = 12.0, 2.6 Hz); 4.04 (H-6, ddd, *J* = 10.0, 10.0, 2.2 Hz); 3.58 (MTPA OCH₃, s); 3.08 (H-2a, t, *J* = 10.5 Hz); 2.77 (H-2b, dd, *J* = 10.7, 3.2 Hz); 2.66 (H-4, m); 2.38 (H-11, overlapped); 2.33 (H-8a, overlapped); 2.25 (H-5a, m); 1.99 (H-8b, dd, *J* = 13.8, 2.6 Hz); 1.88 (H-7, overlapped); 1.88 (H-5b, overlapped); 1.83 (H₃-14, bs); 1.20 (H₃-13, d, *J* = 7.5 Hz); 1.14 (H₃-15, d, *J* = 7.5 Hz); FABMS (glycerol matrix, positive ions) *m/z* 483 [M + H]⁺.

Molecular Modeling Calculations. Molecular modeling calculations were performed on a SGI Origin 200 8XR12000, while graphics were

carried out on SGI Octane 2 and Octane workstations. All the possible ketopelenolides C and D stereoisomers were built using the Insight 2005 Builder module (Accelrys, San Diego, CA). Molecular mechanic (MM) and dynamic (MD) calculations were performed using the atomic potentials and charges assigned by the cff91 force field, while semiempirical calculations were performed using the Mopac 6.0 package. The conformational space of the compounds was sampled through 200 cycles of Simulated Annealing (Discover 3 module, Insight 2005). An initial temperature of 1000 K was applied to the system for 1000 fs with the aim of surmounting torsional barriers; successively temperature was linearly reduced to 300 K with a decrement of 0.5 K/fs (time step = 1.0). The resulting structures were subjected to energy minimization within Insight 2005 Discover 3 module (cff91 force field,¹⁷ Conjugate Gradient algorithm) until the maximum rms derivative was less than 0.001 kcal/Å. All calculations were performed using a CHCl_3 dielectric constant of 4.81. The MD/MM conformers were ranked on the basis of their conformational energy values and grouped into families according to their 10-membered-ring dihedral angle values. Successively, the energetic relative minimum of each family was subjected to a full geometry optimization by semiempirical calculations, using the quantum mechanical method AM1 in the Mopac 6.0 package in the Ampac/Mopac module of Insight 2000.1. GNORM value was set to 0.5. To reach a full geometry optimization, the criterion for terminating all optimizations was increased by a factor of 100, using the keyword PRECISE.

Acknowledgment. Financial support was provided by MIUR-PRIN 2004 (Progetto Chemorecezione Gustativa).

Supporting Information Available: NMR spectra for compounds **2** and **3**, families of conformations for **C1–C4** and **D1–D4**, and details about GIAO calculations of ^{13}C NMR resonances. This material is available free of charge via the Internet at <http://pubs.acs.org>.

References and Notes

- (1) Bifulco, G.; Dambruoso, P.; Gomez-Paloma, L.; Riccio, R. *Chem. Rev.* **2007**, *107*, 3744–3779, and references therein.
- (2) Fattorusso, C.; Stendardo, E.; Appendino, G.; Fattorusso, E.; Luciano, P.; Romano, A.; Tagliatalata-Scafati, O. *Org. Lett.* **2007**, *9*, 2377–2380.
- (3) Appendino, G.; Aviello, G.; Ballero, M.; Borrelli, F.; Fattorusso, E.; Petrucci, F.; Santelia, F. U.; Tagliatalata-Scafati, O. *J. Nat. Prod.* **2005**, *68*, 853–857.
- (4) Fraga, B. M. *Nat. Prod. Rep.* **2004**, *21*, 669–693.
- (5) Bates, R. B.; Cekan, Z.; Prochazka, V.; Herout, V. *Tetrahedron Lett.* **1963**, *17*, 1127–1130.
- (6) Goethers, S.; Imming, P.; Pawlitzki, G.; Hempel, B. *Planta Med.* **2001**, *67*, 292–294.
- (7) Brockhoff, A.; Behrens, A.; Massarotti, A.; Appendino, G.; Meyerhof, W. *J. Agric. Food Chem.* **2007**, *55*, 6236–6243.
- (8) Mazur, Y.; Weizman, A. *J. Am. Chem. Soc.* **1953**, *75*, 3865–3866.
- (9) Masayoshi, A.; Hideki, Y. *J. Org. Chem.* **1993**, *58*, 4127–4131.
- (10) Bates, R. B.; Cheer, C. Y.; Sneath, T. C. *J. Org. Chem.* **1970**, *35*, 3960–3961.
- (11) Wang, W. Z.; Tan, R. X.; Yao, Y. M.; Wang, Q.; Jiang, F. X. *Phytochemistry* **1994**, *37*, 1347–1349.
- (12) Ohtani, I.; Kusumi, T.; Kashman, Y.; Kakisawa, H. *J. Am. Chem. Soc.* **1991**, *113*, 4092–4096.
- (13) Cimino, P.; Gomez-Paloma, L.; Duca, D.; Riccio, R.; Bifulco, G. *Magn. Reson. Chem.* **2004**, *42*, S26–S33.
- (14) Adamo, C.; Barone, V. *J. Chem. Phys.* **1998**, *108*, 664–675.
- (15) Bifulco, G.; Gomez-Paloma, L.; Riccio, R. *Tetrahedron Lett.* **2003**, *44*, 7137–7141.
- (16) Barone, G.; Duca, D.; Silvestri, A.; Gomez-Paloma, L.; Riccio, R.; Bifulco, G. *Chem.–Eur. J.* **2002**, *8*, 3240–3245.
- (17) Maple, J. R.; Hwang, M. J.; Stockfisch, T. P.; Dinur, U.; Waldman, M.; Ewig, C. S.; Hagler, A. T. *J. Comput. Chem.* **1994**, *15*, 162–182.

NP8003547